

Stochastic Coulomb Interactions in space charge limited electron emission

M. D. Nijkerk^{a)}

TNO Institute of Applied Physics, P.O. Box 155, 2600 AD Delft, The Netherlands

P. Kruit

Delft University of Technology, Faculty of Applied Sciences, Lorentzweg 1, 2628 CJ Delft, The Netherlands

(Received 12 January 2004; accepted 7 June 2004)

Emission models that form the basis of self-consistent field computations make use of the approximation that emitted electrons form a smooth space charge jelly. In reality, electrons are discrete particles that are subject to statistical Coulomb interactions. A Monte Carlo simulation tool is used to evaluate the influence of discrete space charge effects on self-consistent calculations of cathode-ray tube optics. We find that interactions in the space charge cloud affect the electron trajectories such that the velocity distribution is Maxwellian, regardless of the current density. Interactions near the emitter effectively conserve the Maxwellian distribution. The surprising result is that the width of the distribution of transversal velocities does not change. The distribution of longitudinal velocities does broaden, as expected from existing theories. © 2004 American Institute of Physics. [DOI: 10.1063/1.1777395]

I. INTRODUCTION

The world's most widely used electron source consists of a flat surface, heated for creating thermal electron emission, with an electric field perpendicular to the surface for accelerating the electrons into a beam. This kind of source is found in cathode-ray tubes (CRTs), electron beam accelerators, and many other scientific instruments. The thermionic emission current density is described by the Richardson-Dushman equation,

$$j = AT^2 \exp(-\phi/k_B T), \quad (1)$$

where A is the universal thermionic constant ($120 \text{ A/cm}^2 \text{ K}^2$), T temperature, ϕ workfunction, and k_B is the Boltzmann constant. Since this is the maximum current density that can come from a cathodes, it is called the saturation current density. The emitted charge may create a repelling space charge cloud in front of the cathode, forcing the slowest electrons back. The resulting state of space charge limited current density can be described by Child's model for a diode configuration in which an infinitely wide flat anode at potential V_d is placed at a distance d from the cathode,

$$j = \frac{4}{9} \epsilon_0 \sqrt{\frac{2e}{m}} \frac{V_d^{3/2}}{d^2}. \quad (2)$$

Child's law was derived assuming zero initial velocity of the electrons. In Langmuir's model, the initial Maxwellian energy distribution is taken into account, leading to the existence of a potential minimum in front of the cathode and a slightly different dependence of the current density on the anode potential. However, there is no simple equation anymore for the dependency and the model must be solved numerically.

For more realistic, but also more complicated geometries than a planar diode, the cathode might be curved or the electric field at the cathode might be position dependent. One way to deal with this is to apply the Langmuir model locally and thus find a local current density and a local distance between the cathode and the potential minimum. The curved plane which contains the minima is considered to be a virtual emitter¹ with a position-dependent current density. In fact, one can take any cross section through an electron beam as a virtual emitter, as long as the distribution of the electrons over angles and position is given correctly, or in other words, as long as the initial conditions at the virtual source plane are consistent with the six-dimensional phase space density at that plane in the beam.

A possible source of inaccuracies in all virtual emitter models is that the space charge is assumed to be a smooth jelly, thus neglecting the discreteness of space charge. The effect of this approximation is twofold. First, the stochastic Coulomb interactions are ignored whereas it is known that the collisions between individual electrons have a pronounced effect on electron beam properties in many situations. Interacting electrons arrive at the target plane with a transversal displacement with respect to noninteracting electrons. This displacement is called trajectory displacement.² A further effect of statistical interactions is the increase in axial velocity width.³ Generally, Coulomb interactions can lead to a decreased resolution of the imaging system. Second, fluctuations in the spatial current distribution known as Poisson fluctuations or shot noise might influence the local space charge repulsion and thus the emission current density. In the space charge limited beam in a typical CRT, the virtual emitter properties are determined by features in the space charge field with a length scale of a few micrometers. In a cube with $1 \mu\text{m}$ size the number of electrons is as low as ten, so statistical fluctuations may well play a role.

The modeling of Coulomb interactions in particle beams

^{a)} Author to whom correspondence should be addressed; FAX: +31-15-2692111; electronic mail: nijkerk@tpd.tno.nl

is well established, both analytically and through Monte Carlo approaches⁴⁻⁷ but the modeling of Coulomb interactions near the emitter is somewhat more complicated. The most obvious problem is that there are many electrons near the cathode surface that do not make it into the beam, but may have interaction with electrons that make it through the potential barrier. A second problem is the local acceleration and deceleration from a strong space charge force: most established models work with a beam in field free space, or at least in a beam with the main velocity component already in the direction of the optical axis. We have written a program that takes all the peculiarities of the emission region into account.⁸ All effects are translated to velocity and spatial distributions in the virtual emitter.

The results of the simulations will be described both for typical current densities in CRTs for televisions and computer monitors and for special application high current sources. Finally, a general consideration of the increase of axial velocity width known from plasma physics is presented and compared to some of the simulation results.

II. RESULTS OF MONTE CARLO SIMULATIONS

We have simulated a planar cathode with temperature $T=1160$ K (0.1 eV/ k_B). The simulation has been performed for a cubic electron box with edge 10 μm which is large enough to encompass the characteristic features of the expected potential distribution. A cubic region of this size in front of an emitter contains ≈ 1000 electrons. To prevent boundary effects in the lateral direction, the model effectively contains an endless array of such boxes.

At the start of the simulation, the electron box is empty. Electrons are being emitted into the box continuously, at a rate corresponding to the saturation current. Apart from the mutual Coulomb interactions, the electrons experience an extracting electric field of $F=-105^5$ V/m. This particular value for the extracting field is chosen such that in the stationary state, current flows both through the end plane in the positive z direction and through the cathode plane in the negative z direction, in other words, the current is space charge limited. After about 0.05 ns a state of equilibrium is reached, that is, there is no systematic change in the total number of particles in the box. The current flowing through the end plane, determined by counting the number of electrons passing the end plane during a short time interval after equilibrium, is 2.74 A/cm². The potential difference between emitter and end plane is 0.32 V.

This result is in agreement with Langmuir's theory if the emission of a 10 μm diode with anode voltage 0.32 V is calculated. These settings yield a space charge minimum $V_m=-0.133$ V at $z_m=2.35$ μm , resulting in a space charge limited current of 2.65 A/cm². The difference with respect to the Monte Carlo current can be explained in terms of numerical noise. Note that in this simulation example the extracting electric field is implemented not by applying a fixed potential of 1 V to the end plane at 10 μm but rather, by exerting a corresponding force locally at the cathode. This is

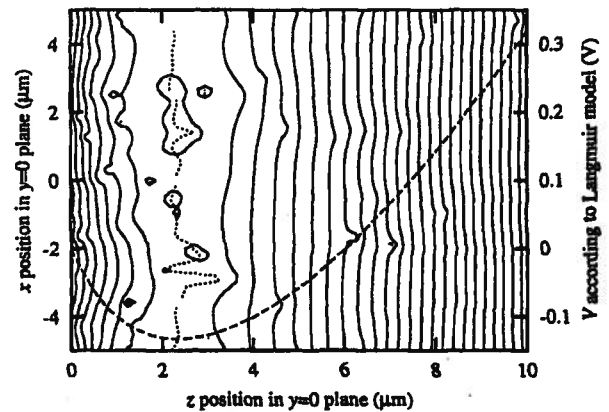


FIG. 1. Stationary space charge potential distribution at the plane $y=0$ (solid equipotential lines), plotted together with the solution according to the Langmuir model (dashed line). The discontinuous dotted line shows the positions of the local potential minima. The deviation from the planar potential distribution due to the discreteness of the electrons is most clearly visible at the potential minimum.

the reason that the potential at the end plane is not fixed but drops from 1 V, when the box is empty, to 0.32 V, when the box is filled with charge.

In Fig. 1 equipotentials of the stationary electron cloud after 0.4 ns are plotted. Instead of a well-defined equipotential line corresponding to the minimum, parallel to the cathode, the minimum plane is a disjunct surface with multivalued potential, indicated with the dotted lines. Note that the local reductions in space charge barrier height do not give rise to a substantial increase in emission current. Thus, there is no reason to modify the Langmuir emission equations.

The velocity distributions at the plane $z=10$ μm are plotted in Fig. 2. The dotted lines correspond to the Maxwellian velocity distributions one would expect in a continuous space charge field without stochastic interactions.

The transversal velocity distribution of the electrons is indistinguishable from a Maxwellian distribution, except for the presence of Monte Carlo noise. In contrast, the axial velocity distribution of the electrons clearly shows a leading edge instead of a discontinuous step.

In order to exaggerate the effects of statistical interac-

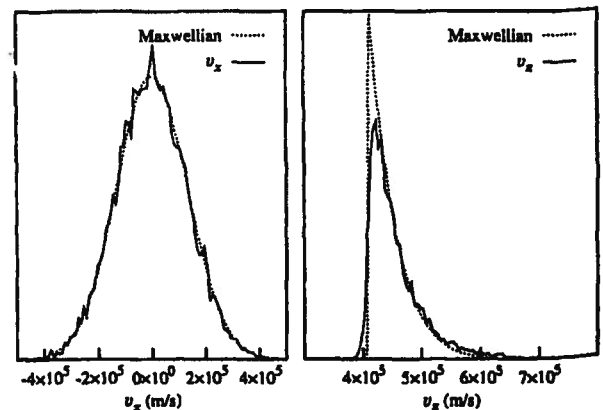


FIG. 2. Velocity distributions at $z=10$ μm (solid lines) for $j_{sat}=10$ A/cm². The dotted lines correspond to the Maxwellian distribution in a continuous space charge cloud.

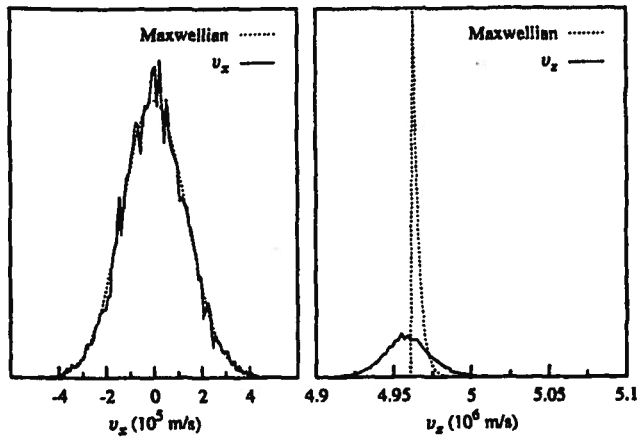


FIG. 3. Velocity distributions for $j_{sat}=10^4$ A/cm².

tions, the current was increased 1000-fold to a value uncharacteristic for CRTs of $j_{sat}=10^4$ A/cm². The applied electric field was increased to 10^7 V/m and the box width was decreased to $0.5 \mu\text{m}$ in order to obtain a sufficiently high space charge limited current and to limit computation time. The results are shown in Fig. 3. The transversal velocity distribution is similar, whereas the axial velocity distribution now deviates significantly from the Maxwellian distribution.

One may be inclined to conclude that statistical Coulomb interactions do not change the transversal velocity component even in situations with current densities as high as 10^4 A/cm². However, this is counterintuitive, considering the fact that Coulomb interactions have changed the axial velocity distribution significantly. It can furthermore easily be checked, for instance by plotting trajectories in the xy plane, that electrons are indeed pushed from their unperturbed paths by their neighbors and Coulomb interactions do, in fact, influence the trajectories.

The notion that Coulomb interactions in the virtual emitter region influence the trajectories of the electrons without affecting the velocity distribution seems contradictory, but it is not. We changed the velocity distribution of emitted electrons at the emission plane artificially from a Maxwellian to a top hat-shaped distribution and saw the Maxwellian veloc-

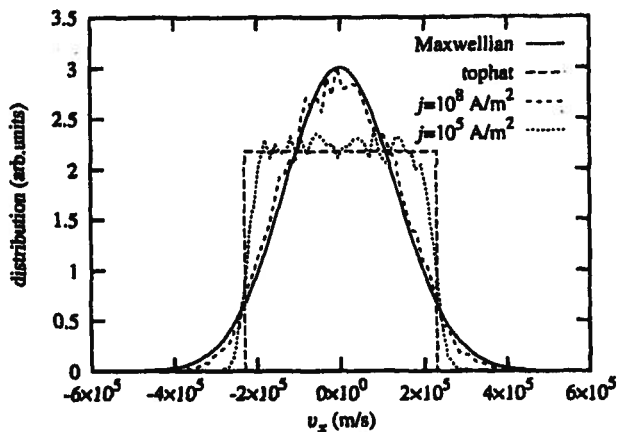


FIG. 4. Transversal velocity distribution at $z=10 \mu\text{m}$ of electrons emitted with a top hat-shaped distribution. When the current density is high, the top hat distribution relaxes towards a Maxwellian. For low currents, the particle cloud becomes too rare for interactions to be noticeable.

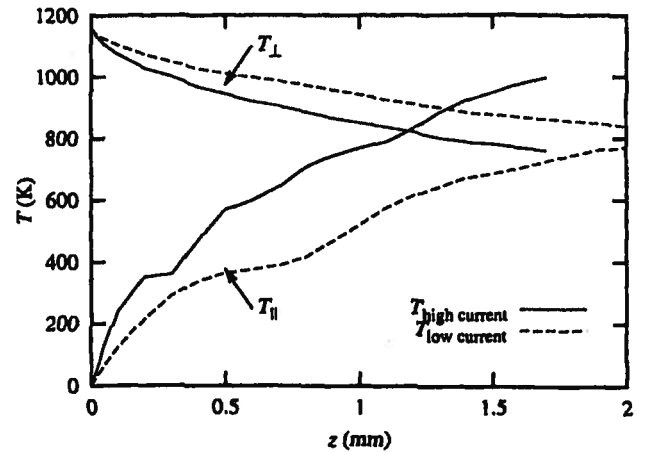


FIG. 5. Graph of the relaxation of transverse and longitudinal beam temperature (T_{\parallel} and T_{\perp}). The curves give the beam temperatures as determined using a Monte Carlo simulation of an electron bunch progressing in field-free space, with current density of $j=1.8 \times 10^7$ A/m² (solid) and 0.9×10^7 A/m² (dashed).

ity distribution reappear when performing the simulation with a current density of 10^4 A/cm² (Fig. 4). Apparently, Coulomb interactions play a role, but their effect is precisely to maintain the Maxwell distribution. This is in agreement with the fact that random interactions bring about a relaxation towards the most probable distribution, which is the Maxwell distribution.

The calculation with a top hat initial velocity distribution was repeated for different current densities. The plots in Fig. 4 show that at low current densities, the velocity distribution stays far from Maxwellian. The fact that at a current density of 10^4 A/cm², which is more realistic for a CRT, the velocity distribution has remained top hatlike, indicates that at current densities for typical CRTs the space charge cloud is too rare to be susceptible to statistical interactions.

Therefore, if a Maxwellian emission distribution at the cathode is assumed, the transversal velocity distribution of the emitted electrons at the virtual emitter of a planar cathode is effectively not influenced by Coulomb interactions in front of the emitter, no matter how high the saturation current density.

If one would try to apply the now well-established equations from Jansen⁴ for trajectory displacement, the first difficulty is the changing acceleration near the cathode. Usually this can be dealt with by using a "slice method," where the contribution from different slices along the z axis are added. However, this does not work in the Gaussian regime and certainly not in the regime between Lorentzian and Gaussian, because some collisions continue between slices, necessitating linear addition of the displacements and some are complete within one slice, necessitating quadrature addition of the displacements. A second problem is that the basis of the theory is the calculation of the distribution of displacements of a set of reference particles on the axis of the system. We would certainly find displacements for the high current densities, and yet we know that the distribution of transversal energies does not change. This is because other particles, which started with a large transversal velocity, end up going

more parallel to the axis. In fact, the transverse velocity distribution can become slightly narrower, as explained in the following section.

III. RELAXATION OF BEAM TEMPERATURE

The concept of relaxation of the velocity distribution towards a Maxwellian distribution as found for the transversal velocities is applicable in the discussion of the axial velocity distribution. Under the influence of an external axial electric field, the axial velocity distribution of the electron cloud is contracted, illustrated in the graphs of the axial velocity distribution in Figs. 2 and 3: the width of the distribution in m/s is smaller for the accelerated beam than for the unaccelerated beam. This is a consequence of the quadratic dependency of the kinetic energy on the particle velocity. Examine the difference in kinetic energy between two particles with axial velocity v_z and $v_z + \Delta v_z$,

$$\Delta E = \frac{1}{2}m(v_z + \Delta v_z)^2 - \frac{1}{2}mv_z^2 \approx mv_z\Delta v_z, \quad (3)$$

when $\Delta v_z \ll v_z$. The acceleration of the two particles traveling a short distance in an electric field leaves their energy difference invariant. The ensuing increase in v_z must be accompanied by a decrease in Δv_z .

We saw that random interactions serve to redistribute the two transversal velocity components individually to an equilibrium distribution. When including the axial component in the consideration of the random exchange of momentum it is useful to regard the electron cloud in the frame of reference moving along with the beam. There is no preferential direction in this frame and the equilibrium velocity distribution is isotropic.

It would be interesting to see how the velocity components redistribute as the beam progresses along the optical axis. To facilitate a more quantitative consideration of relaxation towards equilibrium it is useful to introduce the "beam temperature." The velocity distribution of a particle beam can be specified in terms of an longitudinal and a transverse beam temperature,

$$T_{\parallel} = \frac{m}{k_B} (\langle v_z^2 \rangle - \langle v_z \rangle^2), \quad (4)$$

$$T_{\perp} = \frac{m}{2k_B} (\langle v_x^2 \rangle + \langle v_y^2 \rangle - \langle v_x \rangle^2 - \langle v_y \rangle^2), \quad (5)$$

respectively. Here, $v_i^2 = v_x^2 + v_y^2$. Relaxation of the velocity distributions, as a result of interactions, can now be described via temperature relaxation of the longitudinal and transverse temperature. The longitudinal temperature, like the generic axial velocity spread discussed above, reduces with acceleration.

The present Monte Carlo model can be used to determine the temperature relaxation. Instead of going to a steady-state situation where electrons enter and exit the box continuously, we now follow a finite bunch of particles in a very long particle box at a certain energy and observing its velocity distribution as it is allowed to progress freely along the optical axis.

Before discussing the outcome of the simulation it is informative to analyze the temperature relaxation adopting a theory originally applied to plasma physics. The relaxation between the longitudinal and transverse temperature can be described using the equation⁹

$$\frac{dT_{\perp}}{dt} = -\frac{1}{2} \frac{dT_{\parallel}}{dt} = \frac{T_{\perp} - T_{\parallel}}{\tau}, \quad (6)$$

where the factor 1/2 is due to the fact that T_{\parallel} changes twice as fast as T_{\perp} . Equation (6) defines the relaxation time τ . It is a function of the particle charge and mass, as well as T , T_{\parallel} , and T_{\perp} with¹⁰

$$\frac{1}{\tau} = \frac{8\pi^{1/2}ne^4}{15[4\pi\epsilon_0^2m^{1/2}(k_B T_{\text{eff}})^{3/2}]} \ln \Lambda, \quad (7)$$

where n is the particle density, $\ln \Lambda$ is the Coulomb logarithm,

$$\ln \Lambda = \ln \frac{12\pi(\epsilon_0 k_B T)^{3/2}}{e^3 n^{1/2}}, \quad (8)$$

and the effective temperature T_{eff} is defined through

$$\frac{1}{(T_{\text{eff}})^{3/2}} = \frac{15}{4} \int_{-1}^1 \frac{x^2(1-x^2)dx}{[(1-x^2)T_{\parallel} + x^2T_{\perp}]^{3/2}}. \quad (9)$$

This model has been confirmed experimentally in measurements of anisotropic temperature relaxation in a magnetized plasma.¹¹ In another paper¹² the model has been successfully applied to measurements of Boersch effect in a retarding field energy analyzer.

The present Monte Carlo model was used to simulate the beam temperature relaxation for a bunch of particles. The bunch consisted of 2000 particles with beam energy 80 V forming a sample of initial length 37 μm in an electron box with width 1.6 μm . The particular choice of beam energy and sample length is chosen to correspond to the space charge limited current plotted in Fig. 3, followed by drift space. In view of the excessively high saturation current this is not a realistic physical situation occurring in a CRT but as we have seen above, beam temperature relaxation is scaleable and the results can be adjusted for the application to a CRT. A second computation was performed at the same beam energy and electron box size, with a 50% lower current density, leading to a 50% lower particle density and accordingly to a larger time constant.

Initially, the transverse beam temperature is equal to the cathode temperature and the longitudinal beam temperature is negligible due to the beam acceleration. Advancing along the optical axis, Coulomb collisions cause relaxation of the beam temperatures until equilibrium is reached. According to the plasma theory, at $z=2$ mm, the temperatures differ by 0.5%.

The results of the Monte Carlo simulation are presented in Figs. 5 and 6. The temperature relaxation as predicted by plasma theory can be determined by solving Eq. (6) numerically. In Fig. 5 the two situations with differing particle densities are shown. The difference in time scale is clearly vis-

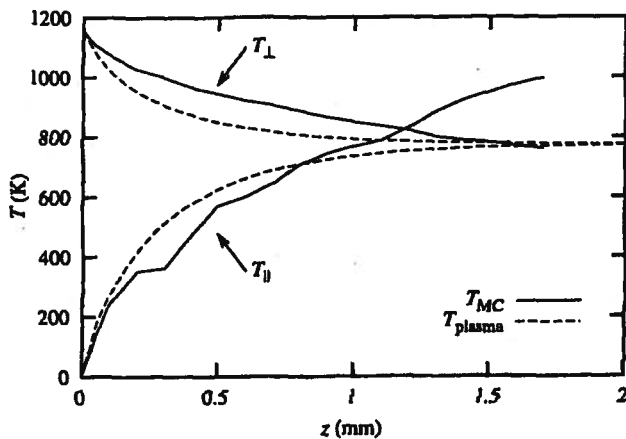


FIG. 6. Comparison with plasma theory. The dashed curve is the solution of the differential equation from plasma theory, the solid curve is the high current Monte Carlo simulation of the Fig. 5.

ible. In Fig. 6 the situation corresponding to high current is plotted together with the temperature relaxation as determined from plasma theory.

The time scale of relaxation is reasonably well reproduced in the simulations. The transverse temperature stays behind somewhat, since the transverse dimensions of the electron bunch are much smaller than the axial dimensions. One would prefer the dimensions to be of equal order but this would result in extremely long computation time. Convergence to equilibrium does not occur in the simulation. The deviations with respect to the theory thus seem to be rather significant. This can be explained by noting that the simulation model is not well suited to simulate a plasma. As a finite particle bunch progresses in drift space along the optical axis, the particle bunch will increase in length due to the initial axial energy spread, as a result of which the particle density will decrease: fast particles move to the front of the bunch while slow particles move to the back, thus no sufficient collisions can take place to cause relaxation. Furthermore, the particles at the front and the back of the bunch feel unbalanced space charge forces, further adding to the incoherence of the particle bunch. It is therefore understandable that the Monte Carlo curves and the plasma model curves are not completely similar.

The fact that the plasma theory is not exactly reproduced by the simulation is not a serious shortcoming considering the applicability to a practical beam. It must also be realized that the plasma theory is not fully applicable to particle beams, see the extensive discussion by Jansen.⁴ One reason is that many collisions between particles are not complete in the time considered and yet this is an assumption of the plasma theory. Another reason is the possibility of potential energy relaxation which is not taken into account: this is

probably not important here, but is dominant in a cylindrical beam segment with all particles originally parallel and of equal energy.

The problem calculated here, an extremely high current beam running unhampered at 80 eV for several millimeters, is not particularly realistic. An electron bunch in the spot forming region of a CRT has to run for 14 km to come to the same level of equilibrium as the fictitious beam achieves at 2 mm. For most particle beams only a very small interval at the left of Fig. 6 is relevant, where the differences between simulation and plasma theory are small. However, cathodes with saturation current density up to 1000 A/cm² have been developed for continuous operation,¹³ and in pulsed operation even higher densities can be reached.

IV. CONCLUSIONS

We have used a simulation tool to take into account all effects relating to discrete space charge in front of a thermionic emitter operating in the space charge regime. Disturbances in the potential distribution due to the discreteness of the charge do not show up in the transversal velocity distribution of the electrons. Statistical Coulomb interactions do not interfere with the Maxwellian transversal velocity distribution. For high current densities there may be a visible effect of the broadened axial velocity distribution known as the Boersch effect. Although these current densities can in practice occur for thermionic emitters, they are applicable to completely different situations than CRT conditions. Reasonable estimates of the energy broadening may be obtained from the theory on relaxation of effective beam temperatures.

ACKNOWLEDGMENT

This work was made possible with financial support of LG. Philips Displays, Eindhoven, The Netherlands.

¹K. R. Spangenberg, *Vacuum Tubes* (McGraw-Hill, New York, 1948) p. 191.

²K. H. Loeffler, Ph.D. thesis, University of Berlin, 1964.

³H. Boersch, *Z. Phys.* **139**, 115 (1954).

⁴G. H. Jansen, *Adv. Electron. Electron Phys.*, Suppl. **21**, 1 (1990).

⁵E. Munro, *Proc. SPIE* **3777**, 215 (1999).

⁶H. Shimoyama, Y. Shimazaki, and A. Tanaka, *Proc. SPIE* **2014**, 99 (1993).

⁷X. Jiang, Ph.D. thesis, Delft University of Technology, 1996.

⁸M. D. Nijkerk, *J. Phys. E* (submitted).

⁹M. Reiser, *Theory and Design of Charged Particle Beams* (Wiley-Interscience, New York, 1994), p. 526.

¹⁰S. Ichimaru and M. N. Rosenbluth, *Phys. Fluids* **13**, 2778 (1970).

¹¹A. W. Hyatt, C. F. Driscoll, and J. H. Malmberg, *Phys. Rev. Lett.* **59**, 2975 (1987).

¹²Y. Zou *et al.*, *Phys. Rev. ST Accel. Beams* **5**, 072801 (2002).

¹³G. Gärtner, P. Geitner, H. Lydtin, and A. Ritz, *Appl. Surf. Sci.* **111**, 11 (1997).